Dieses Dokument ist eine Zweitveröffentlichung (Postprint) /

This is a self-archiving document (accepted version):

David Weyers, Krszystof Nieweglowski and Karlheinz Bock

Advances in UV-lithographic patterning of multi-layer waveguide stack for single mode polymeric RDL

Erstveröffentlichung in / First published in:

Electronics System-Integration Technology Conference (ESTC). Sibiu, 13.-16.09.2022. IEEE, S. 405-409. ISBN 978-1-6654-8947-8.

DOI: https://doi.org/10.1109/ESTC55720.2022.9939517

Diese Version ist verfügbar / This version is available on:

https://nbn-resolving.org/urn:nbn:de:bsz:14-qucosa2-880235

SLUB Wir führen Wissen.

TECHNISCHE UNIVERSITÄT DRESDEN

QUCOSA Quality Content of Saxony

Final edited form was published in "Electronics System-Integration Technology Conference (ESTC). S biu 2022", S. 405 - 409, ISBN 978-1-6654-8947-8
https://doi.org/10.1109/ESTC55720.2022.9939517

Advances in UV-lithographic patterning of multi-layer waveguide stack for single mode polymeric RDL

David Weyers; Krszystof Nieweglowski; Karlheinz Bock

***Abstract*—This paper describes design and advances in process development for UV-lithography of planar single mode waveguides with openings for out-of-plane coupling µ-mirrors. Improvements to multi-layer direct patterning of OrmoCore/-Clad material system using UV-lithography are presented. Near square core cross sections are achieved. However, non uniformity across 4" wafer is shown due to varying proximity and UV-intensity. Openings in full stack with steep sidewalls without residual layer are patterned. Reduction in stack thickness for very small exposure doses due to inhibition even under inert atmosphere is shown. 45°-µ-mirrors are integrated in these openings to manufacture a U-link via a single mode waveguide and two adjacent micro-mirrors. Optical characterization of U-link demonstrates the feasibility of hybrid lithography approach. However, non-uniformity of core cross-section leads to cross coupling of planar waveguides. Outlook to further research on UV-lithography of multi-layer waveguide stack and alignment with µ-mirror printing is given.**

***Keywords*—optical interconnects, single mode, ORMOCER®, hybrid lithography, direct patterning, UV-lithography, 2-photon-polymerization direct-laser-writing, micro-mirrors**

I. Introduction

The ongoing increase in performance and density in high performance computing (HPC) leads to a demand for high IO-bandwidth and bandwidth density. Optical datacom has proven it's superiority for longer distances and plugable transceiver as well as on-board optics are state-of-the-art. Even more so assuring electrical signal integrity for high bandwidth and frequency is increasingly challenging. Thus the optical interconnect is being moved closer to the computing core, culminating in so-called co-package optics approach where photonic processing units (PPU) or receiver and transceiver (Rx/Trx) are integrated on the same interposer with central processing unit (CPU) and high-bandwidth memory (HBM) [1]–[3]. The optical interconnect is then formed via butt-coupling to single mode fibers or fiber arrays aligned in v-grooves. Whilst this is well established and mechanically stable [4], we believe that it also poses as a limit in integration density and scaling as well as costs, due to the needed chip area for v-grooves, , peripheral arrangement on chip/interposer edges and limitation to 1D-arrays. In addition it only provides chip-to-fiber and no chip-to-chip interconnects.

The capability of polymer waveguides (WG) to provide interposer and module level interconnects has been largely demonstrated [5]–[10]. In [11] we proposed a combination of polymer WGs patterned in to an optical redistribution layer (RDL) via UV-lithography and µ-mirrors structured with 2-photon-polymerization direct-laser-writing (2PP-DLW) to provide surface coupling. With the combination of two processes that we termed hybrid lithography we combine the advantages of both. UV-lithography gives parallel, high throughput 2.5D-structuring for the optical RDL. Whilst 2PP-DLW allows for arbitrary 3D-shaped µ-mirrors changing both optical axis and beam shape. This allows for a higher IO-count and integration density compared to fiber butt-coupling. The so-called optical back end of line (BEOL) shown in fig. 1 can be added to an existing electrical interposer to add optical function.

In parallel the fabrication volume of integrated photonics on chip-level, mainly Si- and III-V-photonics is growing rapidly. Coupling to integrated WGs can be provided by tuning the µ-mirrors to match on-chip fiber grating couplers (FGC). In [11] we showed WG stability up to 290 °C making the optical BEOL compatible to standard assembly technologies such as reflow soldering and thermo-compression bonding.

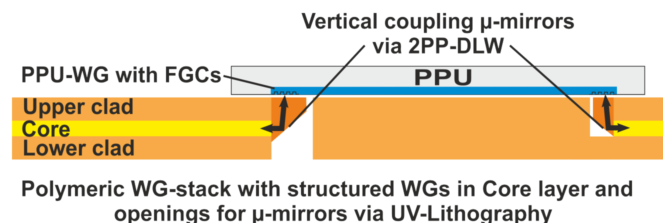

Fig. 1. Schematic of the optical BEOL consisting of polymeric RDL with vertical coupling micro-mirrors used to connect to a PPU with integrated WGs and FGCs.

Whilst an in-depth look at the 2PP-DLW part of hybrid lithography is given in [12], this paper details our recent advances in UV-lithographic multi-layer patterning of the WG stack and integration of µ-mirrors into it.

We first briefly describe the design of WG-stack and µ-mirrors, which we performed detailed in [10].

Secondly we detail our recent advances in UV-lithographic processing and limitations in homogeneity we face with our current tool. We fabricate a U-link by integration µ-mirrors

Provided by Sächsische Landesb bliothek, Staats- und Universitätsbibliothek Dresden

Final edited form was published in "Electronics System-Integration Technology Conference (ESTC). S biu 2022", S. 405 - 409, ISBN 978-1-6654-8947-8
https://doi.org/10.1109/ESTC55720.2022.9939517

in openings in stack.
Thirdly we thoroughly characterize produced samples geometrically and optically. We transmit light across a mirror-WG-mirror U-link as a proof of our hybrid lithography concept.
Finally we conclude our work and discuss aims for future research.

II. Design

The design of our full electro-optical (E/O)-interposer is described in [11], in agreement with that we choose silicon wafers as a substrate for all our tests. In [10] we explained the design of our WGs matching standard single mode fiber as the most common coupling partner and thus also reference for FGCs and other optical elements. Therefore we choose a target core dimension of 7 x 7 μm^2 and numerical aperture (NA) of 0.14. As shown in fig. 2 clad thickness based on simulations in [10] were chosen as 14 µm for bottom and 21 µm top clad which leads to 14 µm above core. Openings for the µ-mirrors could either be structured only in top clad, as shown on the left, or in full stack, as shown on the right. Full stack was chosen since it allows for bigger horizontal mirror extension and reduces impact of sidewall shape deviation via UV-lithography, shown as dashed line. For vertical coupling this sidewall will be covered by the mirror, for but coupling to fiber however the shape affects coupling efficiency. Top clad only opening in contrast would reduce mirror printing time and circumvent reflection effects at silicon surface during µ-mirror printing.

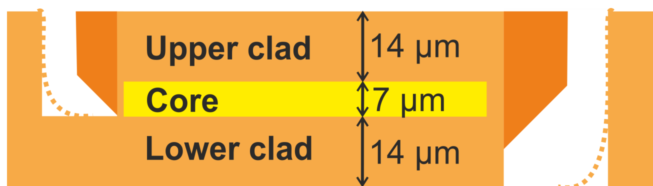

Fig. 2. Layer configuration of full WG-stack with full or top clad only opening for µ-mirrors, integrated µ-mirrors and expexted sidewall shape from UV-lithography as dashed line.

Based on previous experiments which showed issues with adhesion of the µ-mirror, we choose the large 26 x 26 µm mirror footprint in fig. 3, thus anchoring it into the sidewalls of only about 20 µm-wide hole. In addition the larger aperture eases mirror to core alignment. The 10 µm-high base is printed coarsely and with reduced power due to reflection. This is then followed by the 15 µm-high 45°-mirror. Full structure height is set to 35 µm to match the WG-stack Different parameter sets yielding smooth structures in [12] where tested.

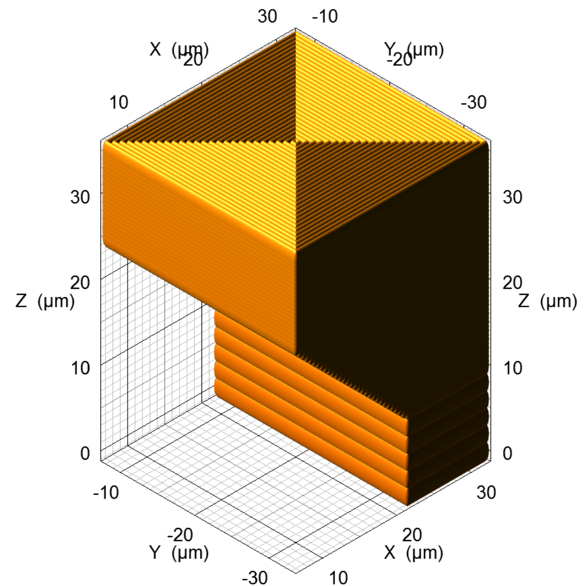

Fig. 3. Used µ-mirror design with large 15 µm x 26 µm aperture and 10 µm high, coarse pedestal.

III. Processing

This section describes our updated polymer WG structuring methods. Thorough process development is described in [10]–[15].

A. UV-Lithography

In [10], [11] we improved our UV-lithographic direct patterning of WGs from multi to single mode dimensions and demonstrated the need for exposure with few µm proximity gap under inter atmosphere to prevent inhibition layers of up to 5 µm and proximity effects. In addition we introduced and explained processing of a metal alignment layer, which is needed for the local alignment of the µ-mirrors. We improved repeatability by reducing UV-intensity to $\approx$ 2.8 mW cm^{-2} to allow for reliable shutter times of $>$ 0.8 s and still yield small doses of 2 to 5 mJ cm^{-2}. UV-intensity is measured using a Thorlabs PM100D power meter with S120VC diode set to 365 nm which has a circular 0.708 cm^2 aperture. Uniformity across a 6” wafer defined as $(PD_{\max} - PD_{\min})/(PD_{\max} + PD_{\min})$ is measured to 2 %.
To manufacture the three layer WG-stack we repeat the flow in tab. I for each layer. A mixture of 70 % OrmoCore and 30 % OrmoClad gives the desired NA of 0.14 [13]. This is diluted 20:1 with OrmoThin, which allows for degassing, syringe application and filtering through 1 µm filter. 14 µm bot clad thickness are yielded with 4 mL of resin applied to the center of a 4” wafer and spun at 5000 RPM. For top clad 5 mL are applied to the entire wafer to prevent shadow effects from WG cores and spun at 2500 RPM. OrmoCore diluted 4:1 with OrmoThin and spun at 3000 RPM is used

Provided by Sächsische Landesb bliothek, Staats- und Universitätsbibliothek Dresden

Final edited form was published in "Electronics System-Integration Technology Conference (ESTC). S biu 2022", S. 405 - 409, ISBN 978-1-6654-8947-8
https://doi.org/10.1109/ESTC55720.2022.9939517

TABLE I
PROCESS FLOW FOR ORMOCORE/-CLAD REPEATED THREE TIMES FOR MULTI-LAYER WG-STACK

Step	Description
1. Resist preparation	Mix by weight ratio, stir 2 h, degas 5 min @ 200 mPa
2. Clean (only Si)	Acetone/IPA/DI-Water spin-clean
3. Surface activation	O_2-Plasma 5 min Si/ 3 min ORMOCER®
4. Reference wafer	4-point contact wafer against mask
5. Spin-coating	Pipette defined volume to center, 30 s @ target RPM, edge beat removal (EBR): spray OrmoThin on edge for last 10 s
6. Soft bake	4 min @ 85 °C on hotplate with N_2-flow
7. Exposure	2 min N_2-flow with 100 µm separation, Alignment with 10 µm separation, Exposure with 1 µm proximity gap
8. Post exposure bake	10 min @ 130 °C on hotplate with N_2-flow
9. Puddle development	30 s each with OrmoDev and IPA, IPA rinse, N_2-blow dry
10. Full exposure	300 s
11. Hard bake full stack	3 h @ 150 °C with 5 K min^{-1} ramp

for the core layer.
For the core layer exposure times from 1.8 to 2.2 s yielded best results. Previous results showed smooth top surfaces but rough sidewalls and a thin adjacent residual layer, depending on exposure dose. Those were structured using 100 nm writing grid wet etched chromium masks. Sidewall roughness might be caused by rough edges in the mask thus we patterned core layers both with 50 nm writing grid wet and 5 nm writing grid dry etched chromium masks.
For the clad layers we focused on steep sidewalls and minimal residual layer at the opening bottom. Due to the low fill factor of the clad masks very low exposure times of 0.9 µs and 0.95 µs for bot and top clad respectively yielded best results, shown in fig. 9a.

B. Micro-Mirror Fabrication with 2PP-DLW

Micro-Mirrors where printed into the openings in WG-stack using 2PP-DLW process, described in detail in [12]. We choose OrmoComp as resin due to its good structuring properties for 2PP-DLW, compatibility to OrmoCore/-Clad and low absorption at the used wavelength of 1310 nm and 1550 nm. We tested two different magnifications for the writing optic, with the 25x allowing for coarser grids, bigger writing window and faster processing. However the lower magnification also reduces the alignment accuracy, which is critical. Thus the 63x optic proved to be more feasible.
During the printing it became clear that the stack thickness was reduced compared to the design goal of 35 µm. Thus pedestal and full height were reduced to 5 µm and 20 µm. In addition overexposure with bubbling occurs at the opening sidewalls, thus scan speed was increased by 25 % and laser power decreased by 10 % to reduce the dose. Since parameters sets with a wide processing window where chosen from [12], these parameter adaptions barely affect the structure quality.

IV. CHARACTERIZATION

In this section we characterize produced samples both geometrically and optically. We highlight and explain deviations as well as possible solutions.

A. Geometrical

Our main focus in process development is reducing WG-attenuation thus we tested different exposure times and intensities. Comparison between identical structures on the same wafer both in the SEM-images in fig. 4 and top view images in fig. 5 clearly shows that a higher deviation than what is to be expected from the uniformity measurements we conducted. Core width is deviating by ±1 µm and a connecting residual layer remains locally. This can not be prevented by further reducing the dose since inhibition will reduce WG-thickness and WG-width will decrease beyond operability. The inter and also some of the intra wafer deviation can be explained by an inaccurate and non uniform proximity gap. We are planning to add spacers to the mask, allowing for exposure in contact mode and a more accurate proximity gap.

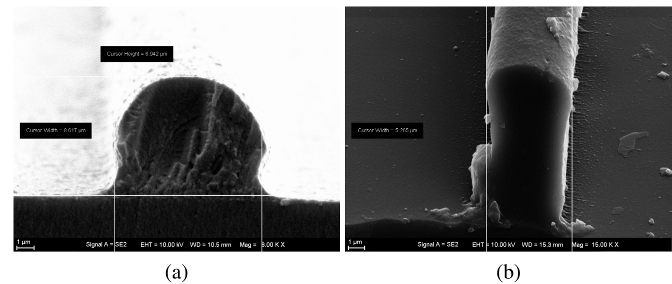

(a) (b)

Fig. 4. SEM images of different achieved cross-sections for 7 µm mask opening with same 5 mJ cm^{-2} dose. Varying local UV-intensity and deviation in proximity distance leads to different cross sections across (a) and (b). Near square shape with extensions at the bottom is achieved in (a), underexposure leads to very narrow wave guide in (b).

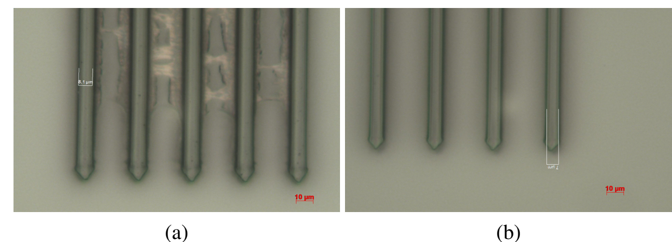

(a) (b)

Fig. 5. Deviation between patterning results in core-layer for same mask opening on one wafer. About 1 µm difference between width in (a) and (b). Visible overexposure and thin connection between WGs in (a).

However, structures that are less than 1 mm apart on the wafer also show these deviations, suggesting that there is a bigger non-uniformity with our exposure system, that we can not capture with the large aperture photo diode. Thus, the dose must be set towards overexposure to prevent WGs in

Provided by Sächsische Landesb bliothek, Staats- und Universitätsbibliothek Dresden

Final edited form was published in "Electronics System-Integration Technology Conference (ESTC). S biu 2022", S. 405 - 409, ISBN 978-1-6654-8947-8
https://doi.org/10.1109/ESTC55720.2022.9939517

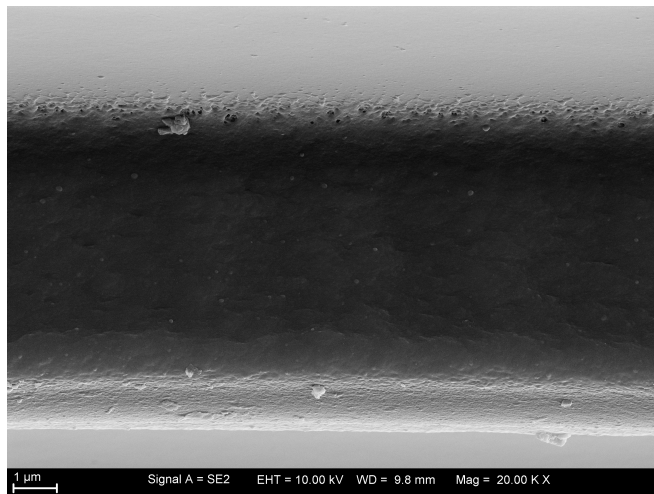

Fig. 6. SEM image of WG sidewall roughness with $50\,\mathrm{nm}$ writing grid wet etched chromium mask. Similar results where achieved with $5\,\mathrm{nm}$ writing grid dry etched chromium mask.

the low intensity zones from lifting off during development. Fig. 6 shows the sidewalls of a WG produced with $50\,\mathrm{nm}$ writing grid wet etched chromium mask. Due to the processing deviations no clear conclusion on an impact of mask quality side wall roughness and attenuation could be derived. The impact of the extend of the residual layer from overexposure is far greater.

With the very low doses for the clad we were able to produce openings without a residual layer and steep sidewalls shown in fig. 7a. The integrated mirror in fig. 7b attaches to sidewall facing the core, core position is vaguely visible in the top right corner of the image. Very good structuring quality was achieved. Only on the top the writing grid is visible due to the reduced exposure dose. Also it is clearly visible that the mirror is higher than the WG-stack. Thickness measurement revealed that the stack is only $10\,\mathrm{\mu m}$ high. This large deviation is being caused by inhibition which occurs even under inert atmosphere for the low exposure doses used.

We will apply different strategies to yield perpendicular openings whilst maintaining the desired stack-up and also to improve core layer structuring homogeneity. First of all the transition to a different exposure system with better proximity control, more homogeneous intensity and improved inert atmosphere is essential. In addition over exposure for the clad openings can be countered by increasing the feature size in mask.

B. Optical

We diced produced planar WG samples and applied optical testing using fiber butt coupling and the setup described in [10], [11]. However, we were unable to surpass the attenuation of $0.64\,\mathrm{dB\,cm^{-1}}$ and $1.5\,\mathrm{dB\,cm^{-1}}$ at $1310\,\mathrm{nm}$ and $1550\,\mathrm{nm}$ respectively we reported in [11]. Therefore we used a InGaAs-beamprofiler to perform near field measurements on five WGs at $40\,\mathrm{\mu m}$ pitch, with light coupled only into the center WG using a SMF28e+ fiber. Fig. 8 clearly shows strong cross coupling caused by the residual layer from overexposure for the $8\,\mathrm{cm}$ long WGs. This again underlines that a high uniformity of exposure dose is mandatory.

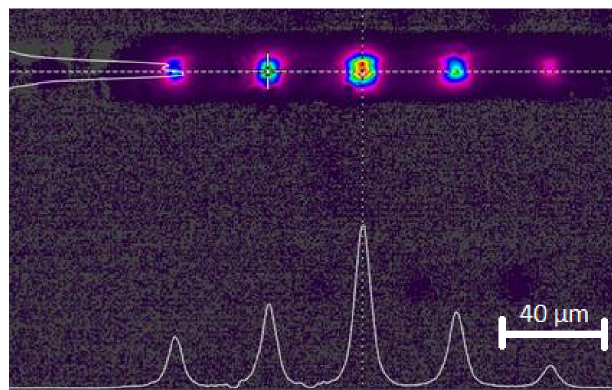

Fig. 8. Power density distribution at $1550\,\mathrm{nm}$ captured with InGaAs NIR-camera showing strong cross coupling. Facet of five $8\,\mathrm{cm}$-long WGs with light coupled only into the center WG is shown.

Finally we used a single mode fiber probe to couple red light through the U-link. Fig. 9 shows the opposing µ-mirror both with and without illumination. This demonstrates the feasibility of our hybrid lithography approach.

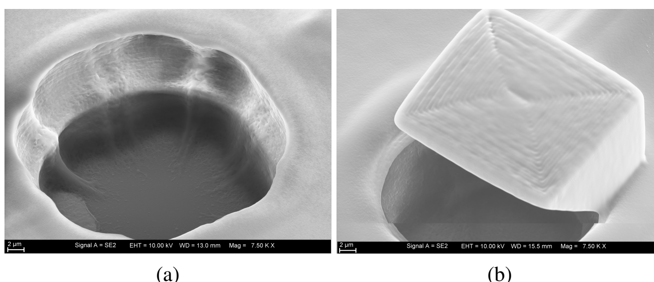

(a) (b)

Fig. 7. SEM images of opening in full stack (a) and opening with integrated µ-mirror (b). µ-mirror extending above WG-stack since it being thinner due to inhibition .

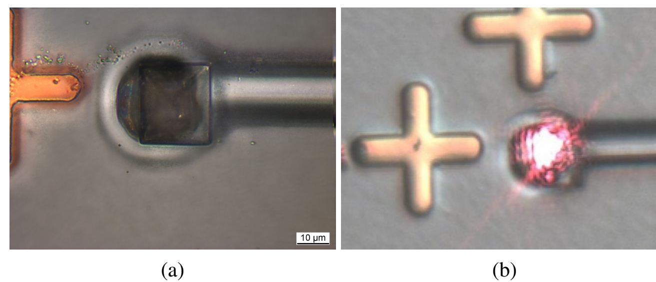

(a) (b)

Fig. 9. Multi focus image of full stack with opening, metal alignment marks, visible core and integrated µ-mirror in (a). Same structure with µ-mirror illuminated via fiber coupling into the mirror at other WG end.

Provided by Sächsische Landesb bliothek, Staats- und Universitätsbibliothek Dresden

Final edited form was published in "Electronics System-Integration Technology Conference (ESTC). S biu 2022", S. 405 - 409, ISBN 978-1-6654-8947-8
https://doi.org/10.1109/ESTC55720.2022.9939517

V. Conclusion and Outlook

We presented our optical BEOL-approach consisting of an optical RDL with vertical coupling elements to FGCs or other surface emitters/receivers. We improved our UV-lithographic patterning of OrmoCore/-Clad material system and demonstrated multi-layer WG-stack with planar, straight single mode WGs and opening for integration of coupling elements via 2PP-DLW. However, exposure dose requirements are at the edge or beyond our tools capabilities. Still we were able to proof our hybrid lithography concept by demonstrating light transmission across a U-link consisting of a planar WG via UV-lithography and two adjacent µ-mirrors via 2PP-DLW.

For future work we will focus on further improving lithographic patterning to meet our goal of WGs with $40\,\mu\text{m}$ pitch on 8” wafer scale with high yield and low attenuation. In addition patterning of vertical facets in clad and proximity effect on WG-end for edge coupling, will be studied. Beam shape will be characterized and design eventually adapted to match respective coupling partners. More complex elements such as bends, crossings and tapers will be patterned and analyzed.
Aspects related to the integration on to the E/O-interposer, such as planarization of copper RDL with the bottom clad layer and impact of underlying electrical lines on WG-attenuation will be studied.
2PP-DLW part of hybrid lithography has proven the capability for simple plane mirrors. Future work will focus on adaption to FGCs and introducing beam shaping function to relax alignment requirements during assembly.

Acknowledgment

This Work has been supported by Germany’s Federal Ministry of Education and Research (BMBF) within the project VE-Silhouette. The authors would like to thank I. Sotiriou for his extensive processing work.

References

[1] M.-J. Lu, S.-Y. Mu, C.-S. Cheng, and J. Chen, “Advanced packaging technologies for co-packaged optics,” in *Proc. of IEEE 72nd Electronic Components and Technology Conf. (ECTC)*. San Diego, CA, USA: IEEE, 2022, pp. 38–42.

[2] B. Chou, B. M. Sawyer*, G. Lyu, E. Timurdugan, C. Minkenberg, A. J. Zilkie, and D. McCann, “Demonstration of fan-out silicon photonics module for next generation co-packaged optics(cpo) application,” in *Proc. of IEEE 72nd Electronic Components and Technology Conf. (ECTC)*. San Diego, CA, USA: IEEE, 2022, pp. 394–402.

[3] S. B. N. Gourikutty, M. C. Jong, C. V. Kanna, D. S. W. Ho, S. W. Wei, S. L. P. Siang, J. Wu, T. G. Lim, R. Mandal, J. T.-Y. Liow, and S. B. 1, “A novel packaging platform for high-performance optical engines in hyperscale data center applications,” in *Proc. of IEEE 72nd Electronic Components and Technology Conf. (ECTC)*. San Diego, CA, USA: IEEE, 2022, pp. 422–427.

[4] A. Janta-Polczynski and M. Robitaille, “Optical fiber pigtails integration in co-package,” in *Proc. of IEEE 72nd Electronic Components and Technology Conf. (ECTC)*. San Diego, CA, USA: IEEE, 2022, pp. 410–422.

[5] Z. Zhang, D. Felipe, V. Katopodis, P. Groumas, C. Kouloumentas, H. Avramopoulos, J.-Y. Dupuy, A. Konczykowska, A. Dede, A. Beretta, A. Vannucci, G. Cangini, R. Dinu, D. Schmidt, M. Moehrle, P. Runge, J.-H. Choi, H.-G. Bach, N. Grote, N. Keil, and M. Schell, “Hybrid photonic integration on a polymer platform,” *Photonics*, vol. 2, no. 3, pp. 1005–1026, 9 2015. [Online]. Available: http://www.mdpi.com/2304-6732/2/3/1005

[6] E. Bosman, G. V. Steenberge, A. Boersma, S. Wiegersma, P. Harmsma, M. Karppinen, T. Korhonen, B. J. Offrein, R. Dangel, A. Daly, M. Ortsiefer, J. Justice, B. Corbett, S. Dorrestein, and J. Duis, “Scalable electro-photonic integration concept based on polymer waveguides,” in *Optical Interconnects XVI*, H. Schröder and R. T. Chen, Eds. SPIE, mar 2016.

[7] L. Ma, X. Xu, and Z. He, “Single-mode polymer waveguides and devices for high-speed on-board optical interconnect application,” in *Optical Interconnects XIX*, H. Schröder and R. T. Chen, Eds. SPIE, mar 2019.

[8] T. Barwicz, A. Janta-Polczynski, S. Takenobu, K. Watanabe, R. Langlois, Y. Taira, K. Suematsu, H. Numata, B. Peng, S. Kamlapurkar, S. Engelmann, P. Fortier, and N. Boyer, “Advances in interfacing optical fibers to nanophotonic waveguides via mechanically compliant polymer waveguides,” *IEEE Journal of Selected Topics in Quantum Electronics*, vol. 26, no. 2, pp. 1–12, mar 2020.

[9] M. Hiltunen, M. T. Harjanne, T. Vehmas, B. Wälchli, P. Heimala, and T. Aalto, “Polymer interposer for efficient light coupling into 3 μm silicon-on-insulator waveguides,” in *Optical Interconnects XX*, H. Schröder and R. T. Chen, Eds. SPIE, feb 2020.

[10] D. Weyers, K. Nieweglowski, L. Lorenz, and K. Bock, “Analysis of polymeric singlemode waveguides for inter-system communication,” in *2021 23rd European Microelectronics and Packaging Conference & Exhibition (EMPC)*. IEEE, sep 2021.

[11] D. Weyers, A. Mistry, K. Nieweglowski, and K. Bock, “Hybrid lithography approach for single mode polymeric waveguides and out-of-plane coupling mirrors,” in *Proc. of IEEE 72nd Electronic Components and Technology Conf. (ECTC)*. San Diego, CA, USA: IEEE, 2022, pp. 1919–1926.

[12] A. Mistry, D. Weyers, K. Nieweglowski, and K. Bock, “Out-of-plane mirrors for single-mode polymeric rdl using direct laser writing,” in *Proc. of 9th Electronic System-Integration Technology Conference (ESTC)*. Sibiu, Romania: IEEE, 2022.

[13] K. Nieweglowski, R. Rieske, S. Sohr, and K.-J. Wolter, “Design and optimization of planar multimode waveguides for high speed board-level optical interconnects,” in *Proc. IEEE 63rd Electronic Components and Technology Conf. (ECTC)*. TU Dresden, 2013, pp. 1898–1904.

[14] L. Lorenz, S. Sohr, R. Rieske, K. Nieweglowski, T. Zerna, and K. . J. Wolter, “Development of a wafer-level integration technology for photonic transceivers based on planar lightwave circuits,” in *Proc. of 37th International Spring Seminar on Electronics Technology (ISSE)*. TU Dresden, 2014, pp. 130 – 136. [Online]. Available: http://ieeexplore.ieee.org/stamp/stamp.jsp?tp=&arnumber=6887578

[15] *Technical Data Sheet - SYLGARD 184 Silicone Elastomer*, Dow Chemical Company.

Provided by Sächsische Landesb bliothek, Staats- und Universitätsbibliothek Dresden